APPLIED PHYSICS LETTERS VOLUME 85, NUMBER 11 13 SEPTEMBER 2004

Properties of MgB_2 thin films with carbon doping

A. V. Pogrebnyakov[a] and X. X. Xi
Department of Physics, Department of Materials Science and Engineering and Materials Research Institute, The Pennsylvania State University, University Park, Pennsylvania 16802

J. M. Redwing, V. Vaithyanathan, D. G. Schlom, and A. Soukiassian
Department of Materials Science and Engineering and Materials Research Institute, The Pennsylvania State University, University Park, Pennsylvania 16802

S. B. Mi and C. L. Jia
Institut für Festkörperforschung, Forschungszentrum Jülich GmbH, D-52425 Jülich, Germany

J. E. Giencke and C. B. Eom
Department of Materials Science and Engineering and Applied Superconductivity Center, University of Wisconsin, Madison, Wisconsin 53706

J. Chen, Y. F. Hu, Y. Cui, and Qi Li
Department of Physics and Materials Research Institute, The Pennsylvania State University, University Park, Pennsylvania 16802

(Received 29 March 2004; accepted 15 June 2004)

We have studied structural and superconducting properties of MgB_2 thin films doped with carbon during the hybrid physical-chemical vapor deposition process. A carbon-containing precursor metalorganic bis(methylcyclopentadienyl)magnesium was added to the carrier gas to achieve carbon doping. As the amount of carbon in the film increases, the resistivity increases, T_c decreases, and the upper critical field increases dramatically as compared to clean films. The self-field J_c in the carbon doped film is lower than that in the clean film, but J_c remains relatively high to much higher magnetic fields, indicating stronger pinning. Structurally, the doped films are textured with columnar nano-grains and highly resistive amorphous areas at the grain boundaries. The carbon doping approach can be used to produce MgB_2 materials for high magnetic-field applications. © *2004 American Institute of Physics*. [DOI: 10.1063/1.1782258]

The 39 K superconductor MgB_2[1] has attracted tremendous interest for its potential in high magnetic-field applications. In particular, high critical current density J_c near the depairing limit has been observed in MgB_2,[2] and unlike high temperature superconductors grain boundaries in MgB_2 do not behave like weak links.[3] Although clean MgB_2 shows low upper critical field H_{c2},[4] in high resistivity MgB_2 films H_{c2} is substantially higher;[5] the critical current density J_c in clean MgB_2 is suppressed quickly by magnetic field,[6] but defects and impurities have been shown to enhance pinning.[7,8] Recently, we have developed a hybrid physical-chemical vapor deposition (HPCVD) technique which produces *in situ* epitaxial MgB_2 films with T_c above 40 K.[10] Because of the highly reducing H_2 ambient and the high purity B_2H_6 source used in the HPCVD process, the technique produces very clean MgB_2 thin films. In this letter, we describe the properties of HPCVD MgB_2 films doped with carbon. The H_{c2} values in these "dirtier" films are significantly higher and the vortex pinning is significantly stronger than those in the clean films.

In situ epitaxial growth of MgB_2 films by HPCVD has been described in detail previously.[9] For carbon doping, we added bis(methylcyclopentadienyl)magnesium [$(MeCp)_2Mg$], a metalorganic magnesium precursor, to the carrier gas of 300 sccm hydrogen at 100 Torr. The flow of the boron precursor gas, 1000 ppm diborane (B_2H_6) in H_2, was kept at 150 sccm. A secondary hydrogen flow was passed through the $(MeCp)_2Mg$ bubbler which was held at 760 Torr and 21.6 °C to transport $(MeCp)_2Mg$ to the reactor. The amount of carbon doping depends on the secondary hydrogen flow rate through the $(MeCp)_2Mg$ bubbler, which was varied between 25 and 200 sccm to vary the flow rate of $(MeCp)_2Mg$ into the reactor from 0.0065 to 0.052 sccm. The chemical compositions of a series of films were determined by wavelength dispersive x-ray spectroscopy to establish a correlation between the carbon concentrations in the films and the hydrogen flow rates through the $(MeCp)_2Mg$ bubbler. The nominal atomic concentrations determined by this approach are used as the carbon concentrations presented in this letter. The films were deposited on (001) 4H–SiC substrates at 720 °C. The thickness of the films was around 2000 Å.

The resistivity (in log scale) versus temperature curves for MgB_2 films with different carbon doping levels are shown in Fig. 1(a). The carbon doping causes a dramatic increase in the resistivity, whereas the T_c of the film is suppressed much more slowly. For example, with a carbon concentration of 24 at. %, the residual resistivity increases from the undoped value of less than 1 $\mu\Omega$ cm to $\sim$200 $\mu\Omega$ cm, but T_c only decreases from over 41 to 35 K. The dependencies of residual resistivity and T_c on the carbon concentration in the doped MgB_2 films are plotted in Fig. 1(b). T_c is suppressed to below 4.2 K at a nominal carbon concentration of 42 at. % when the residual resistivity is 440 mΩ cm. This is very different from those in carbon-doped single crystals, where T_c is suppressed to 2.5 K at a residual resistivity of 50 $\mu\Omega$ cm when 12.5 at. % of carbon is doped into MgB_2.[11] This discrepancy indicates that only a small portion of the carbon in the films is doped into the MgB_2 structure and the

[a]Electronic mail: avp11@psu.edu

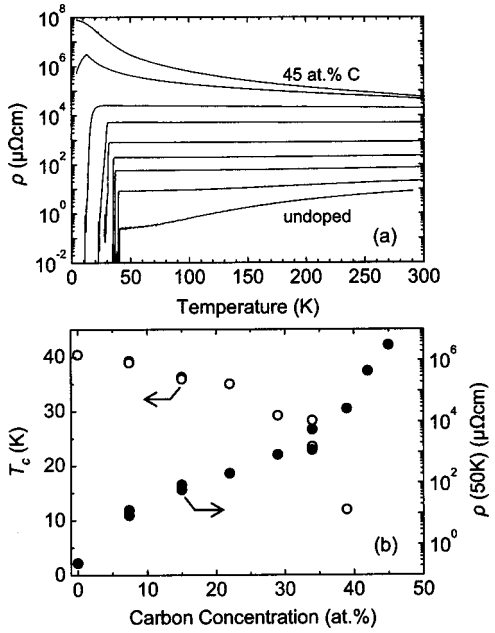

FIG. 1. (a) Resistivity vs temperature curves for MgB_2 films of different carbon doping. (b) Residual resistivity (closed circles) and T_c (open circles) as a function of carbon concentration for films plotted in (a). In (a), from bottom to top, the nominal carbon concentrations of the curves are 0, 7.4, 15, 22, 29, 34, 39, 42, and 45 at. %.

rest most likely forms high resistance grain boundaries giving rise to poor connectivity of the $Mg(B_{1-x}C_x)_2$ grains.[12]

The granular structure of the carbon-doped MgB_2 films is confirmed by TEM. Figure 2(a) is a cross-sectional TEM image of a film with 22 at. % nominal carbon concentration taken along the $[\bar{1}10]$ direction of the substrate. It shows that the film consists of columnar nano-grains (the contrast changes laterally, but not vertically) of $Mg(B_{1-x}C_x)_2$ with a preferential *c*-axis orientation. The selected area electron diffraction pattern taken from the MgB_2/SiC interface area in Fig. 2(b) shows two types of features, diffraction spots and arcs. The spots belong to the single crystal SiC substrate (SC) and the arcs to the MgB_2 film (MB). The arcs consist of many fine spots originating from individual columnar grains which show a deviation of their *c* axis from the film normal.

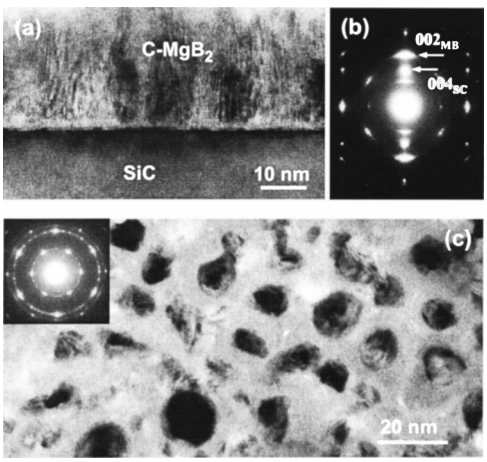

FIG. 2. TEM results of a film with 22 at. % nominal carbon concentration. (a) Cross-sectional image taken along the $[\bar{1}10]$ direction of the substrate. (b) Selected area electron diffraction taken from the MgB_2/SiC interface area. (c) Planar-view image showing nano-grains of carbon doped MgB_2 and an amorphous phase between the grains. The insert is the select area electron diffraction pattern taken along the film normal.

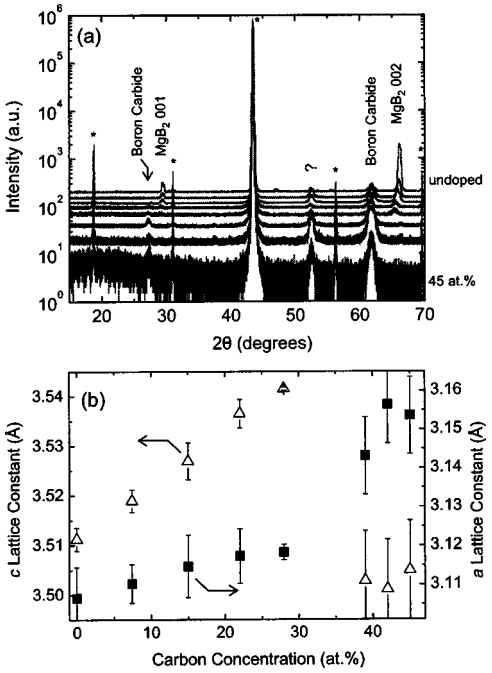

FIG. 3. (a) X-ray diffraction θ–2θ scans for MgB_2 films with carbon doping. From top to bottom, the nominal carbon concentrations are 0, 7.4, 15, 22, 28, 39, 42, and 45 at. %. The spectra are shifted vertically for clarity. The peaks labeled with an asterisk are due to the SiC substrate peaks. (c) The *c*-axis lattice constant (open triangles) and *a*-axis lattice constant (closed squares) of the carbon doped MgB_2 films as a function of nominal carbon concentration.

In the planar-view image in Fig. 2(c), the change of contrast indicates an equiaxial in-plane morphology of the columnar grains, and an amorphous phase is also observed between the grains. We were not able to determine the composition of the amorphous areas, but it is most likely that the large portion of carbon that is not doped into MgB_2 is contained in these areas. The insert in Fig. 2(c) is a typical diffraction pattern taken along the film normal. The strong hexagonal-distributed spots show that the hexagonal-on-hexagonal in-plane relationship between the columnar grains and SiC dominates, while the diffraction rings reveal grains that are randomly in-plane oriented.

Figure 3(a) shows θ–2θ scans of an undoped MgB_2 film and films doped with different amounts of carbon. Compared to the undoped films, the MgB_2 00*l* peaks are suppressed as carbon concentration increases, and dramatically when the carbon concentration is above ~30 at. %. Meanwhile, as shown in Fig. 3(b), both the *c* and *a* axes expand until about 30 at. %, above which the *c* lattice constant decreases and the *a* lattice constant increases dramatically. This behavior is different from that in carbon-doped single crystals, where the *a* axis lattice constant decreases but that of *c* axis remains almost constant for all the carbon concentration.[11] The peak marked by "?" is likely 101 MgB_2, the most intense diffraction peak of MgB_2. It becomes stronger as the carbon concentration increases, indicating an increased presence of randomly oriented MgB_2. The peaks marked by "boron carbide," according to extensive pole figure analysis, are most likely due to B_4C, B_8C, or $B_{13}C_2$. Their intensities also increase with carbon concentration. From the TEM and x-ray diffraction results, we conclude that below about 30 at. %, a small portion of carbon is doped into the $Mg(B_{1-x}C_x)_2$ columnar, *c*-axis-oriented nano-grains, and the rest goes into the grain boundaries consisting of highly resistive amor-

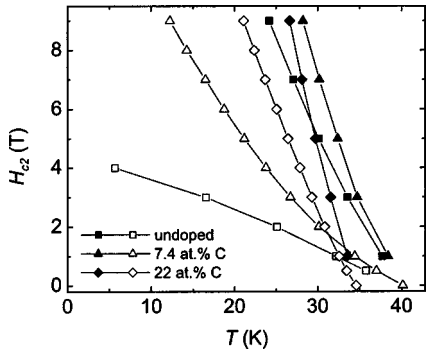

FIG. 4. Upper critical field as a function of temperature for an undoped film and two doped films with 7.4 at. % and 22 at. % nominal carbon concentrations, respectively. The closed symbols are for parallel field ($H_{c2}^{\parallel}$) and the open symbols are for perpendicular field ($H_{c2}^{\perp}$).

phous phases or boron carbides. Above about 30 at. %, the $Mg(B_{1-x}C_x)_2$ nano-grains are completely separated from each other by highly resistive phases, become more randomly oriented, and their lattice constants relax. This is consistent with the result in Fig. 1(b).

The upper critical field H_{c2} was measured using a Quantum Design PPMS system with a 9 T superconducting magnet. Figure 4 shows the results for an undoped, 7.4 at. %, and 22 at. % carbon doped films. The value of H_{c2} is defined by 50% of the normal-state resistance $R(H_{c2})=0.5R(T_c)$. It can be clearly seen that carbon doping changes the downward curvature in $H_{c2}^{\perp}(T)$ for the undoped film to an upward curvature in the carbon doped films. Both the slope, dH_{c2}/dT, near T_c and the low temperature H_{c2} increase with carbon concentration. In high magnetic field measurements, Braccini *et al.* have shown that carbon-doped MgB_2 films as described here have extraordinary $H_{c2}(0)$ values as high as 70 T.[13] The transport $J_c(H)$ at different temperatures, determined by a 1 μV criterion from 20–50 μm bridges, for an undoped and a carbon doped MgB_2 film are shown in Fig. 5.

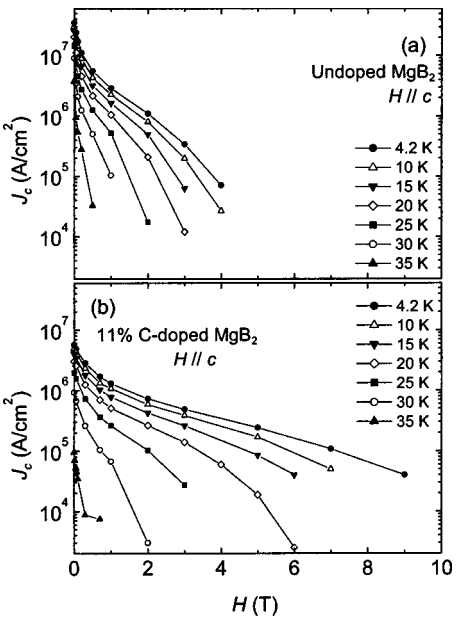

FIG. 5. Critical current density as a function of magnetic field ($\mathbf{H} \| c$) and temperature for (a) an undoped film and (b) a film doped with with 11 at. % nominal carbon concentration.

While the undoped film has high self-field critical current densities, they are suppressed quickly by magnetic field due to the weak pinning. For the film doped with 11 at. % nominal carbon concentration, J_c values are relatively high in much higher magnetic fields. This indicates a significantly enhanced vortex pinning in carbon doped MgB_2 films.

In conclusion, MgB_2 thin films were doped with carbon by adding bis(cyclopentadienyl)magnesium to the carrier gas during the HPCVD process. The residual resistivity increases rapidly while T_c decreases much more slowly with carbon doping. Structural analyses show that only part of the carbon is doped into the MgB_2 lattice and the rest forms highly resistive foreign phases in the grain boundaries. $H_{c2}(T)$ and its slope near T_c increase dramatically as compared to the clean films, which is consistent with the multiband superconductor model of Gurevich and indicates a dirtier π band upon carbon doping.[14] The critical current density in magnetic field increases markedly from that in the clean film due to stronger vortex pinning.

The work is supported in part by ONR under grant Nos. N00014-00-1-0294 (X.X.X.) and N0014-01-1-0006 (J.M.R.), by NSF under grant Nos. DMR-0306746 (X.X.X. and J.M.R.), DMR-9876266 and DMR-9972973 (Q.L.), and through the MRSEC for Nanostructure Materials (C.B.E.), and by DOE under grant No. DE-FG02-03ER46063 (D.G.S.).

[1] J. Nagamatsu, N. Nakagawa, T. Muranaka, Y. Zenitani, and J. Akimitsu, Nature (London) **410**, 63 (2001).
[2] S. Y. Xu, Q. Li, E. Wertz, Y. F. Hu, A. V. Pogrebnyakov, X. H. Zeng, X. X. Xi, and J. M. Redwing, Phys. Rev. B **68**, 224501 (2003).
[3] D. C. Larbalestier, L. D. Cooley, M. O. Rikel, A. A. Polyanskii, J. Jiang, S. Patnaik, X. Y. Cai, D. M. Feldmann, A. Gurevich, A. A. Squitieri, M. T. Naus, C. B. Eom, E. E. Hellstrom, R. J. Cava, K. A. Regan, N. Rogado, M. A. Hayward, T. He, J. S. Slusky, P. Khalifah, K. Inumaru, and M. Haas, Nature (London) **410**, 186 (2001).
[4] P. C. Canfield and G. Crabtree, Phys. Today **56**, 34 (2003).
[5] A. Gurevich, S. Patnaik, V. Braccini, K. H. Kim, C. Mielke, X. Song, L. D. Cooley, S. D. Bu, D. M. Kim, J. H. Choi, L. J. Belenky, J. Giencke, M. K. Lee, W. Tian, X. Pan, A. Siri, E. E. Hellstrom, C. B. Eom, and D. Larbalestier, Supercond. Sci. Technol. **17**, 278 (2004).
[6] X. H. Zeng, A. V. Pogrebnyakov, M. H. Zhu, J. E. Jones, X. X. Xi, S. Y. Xu, E. Wertz, Q. Li, J. M. Redwing, J. Lettieri, V. Vaithyanathan, D. G. Schlom, Z. K. Liu, O. Trithaveesak, and J. Schubert, Appl. Phys. Lett. **82**, 2097 (2003).
[7] Y. Bugoslavsky, G. K. Perkins, X. Qi, L. F. Cohen, and A. D. Caplin, Nature (London) **410**, 563 (2001).
[8] C. B. Eom, M. K. Lee, J. H. Choi, L. Belenky, X. Song, L. D. Cooley, M. T. Naus, S. Patnaik, J. Jiang, M. O. Rikel, A. A. Polyanskii, A. Gurevich, X. Y. Cai, S. D. Bu, S. E. Babcock, E. E. Héllstrom, D. C. Larbalestier, N. Rogado, K. A. Regan, M. A. Hayward, T. He, J. S. Slusky, K. Inumaru, M. Haas, and R. J. Cava, Nature (London) **411**, 558 (2001).
[9] X. H. Zeng, A. V. Pogrebnyakov, A. Kotcharov, J. E. Jones, X. X. Xi, E. M. Lysczek, J. M. Redwing, S. Y. Xu, Q. Li, J. Lettieri, D. G. Schlom, W. Tian, X. Q. Pan, and Z. K. Liu, Nat. Mater. **1**, 35 (2002).
[10] A. V. Pogrebnyakov, J. M. Redwing, J. E. Jones, X. X. Xi, S. Y. Xu, Q. Li, V. Vaithyanathan, and D. G. Schlom, Appl. Phys. Lett. **82**, 4319 (2003).
[11] S. Lee, T. Masui, A. Yamamoto, H. Uchiyama, and S. Tajima, Physica C **397**, 7 (2003).
[12] J. Rowell, Supercond. Sci. Technol. **16**, R17 (2003).
[13] V. Braccini, A. Gurevich, J. Giencke, M. Jewell, C. Eom, D. Larbalestier, A. Pogrebnyakov, Y. Cui, B. T. Liu, Y. F. Hu, J. M. Redwing, Q. Li, X. X. Xi, R. Singh, R. Gandikota, J. Kim, B. Wilkens, N. Newmann, J. Rowell, B. Moeckly, V. Ferrando, C. Tarantini, D. Marr, M. Putti, C. Ferdeghini, R. Vaglio, and E. Haanappel (unpublished).
[14] A. Gurevich, Phys. Rev. B **67**, 184515 (2003).